Fabrication of Micrometer-Scale, Patterned Polyhedra by Self-Assembly**

By *David H. Gracias*, *Vikram Kavthekar*, *J. Christopher Love*, *Kateri E. Paul*, and *George M. Whitesides**

We recently proposed and demonstrated a strategy for fabricating self-assembling, three-dimensional (3D) electrical networks.[1] In this demonstration, we used millimeter scale building blocks (polyhedra) whose faces were patterned with copper connectors and devices (light-emitting diodes). One significant hurdle to implementing self-assembly in practical systems is that of miniaturizing the assemblies. To do so would require us to construct building blocks similar to those of ~1 mm scale,[1] but on the micrometer scale. The building blocks must have the following characteristics: a) polyhedral structures, b) faces patterned with arbitrary patterns that would serve as connectors, and c) microelectronic devices attached to the faces of the polyhedron.

It is difficult to fabricate micrometer scale polyhedral structures. Structures with these dimensions are usually fabricated by projection lithography,[2] and this technique is inherently planar. Most methods of fabrication in 3D utilize processes such as surface micromachining[3] that are precise and versatile, but also expensive and limited in the range of materials that can be used and the types of structures that can be generated. It is also difficult to generate arbitrarily patterned structures in 3D or on curved surfaces. Techniques for patterning have been limited to microcontact printing,[4–6] projection lithography on spherical substrates using elaborate optics,[7] and shell plating onto die-cast mandrills.[8] Fabricating devices on 3D objects is extremely difficult; this is because processes (e.g., ion implantation) used to build silicon-based microdevices[9] are inherently planar techniques.

This paper describes the fabrication of patterned polyhedra, having 100–300 μm sides, by the spontaneous folding of two-dimensional (2D) structures under the influence of the surface tension of liquid solder. Our examination of this approach was stimulated by the early work of Pister[10] and Shimoyama[11] on micromachined hinges and by the extensive research of Syms and others on the use of capillary forces in liquid solder[12–17] and similar methods for directly shrinking polymer joints[18–20] for the assembly of non-planar microstructures. The structures we describe can be patterned and processed in 2D using conventional techniques—photolithography, evaporation, electrodeposition, etching—that have been extensively developed by the semiconductor industry.[9] In the past, auto-folding[12–16] has been used primarily to actuate micrometer scale components in microelectromechanical systems (MEMS) devices. In our work, we demonstrate that the self-assembling process of auto-folding can be used as a strategy for fabricating patterned 3D components from 2D precursors. We have also demonstrated that it is possible to build 3D polyhedra whose faces contain single crystal silicon chips—the most primitive electronic device, i.e., a resistor.

The approach we demonstrate has four steps: 1) The desired structures are designed in planar form as a series of unconnected but adjacent faces. 2) The faces are fabricated in 2D on a sacrificial layer using a combination of photolithography, evaporation, etching, and electrodeposition. 3) The ensemble of faces is covered with a thin film of liquid solder by dip coating. 4) The structure is released from the substrate by dissolving the sacrificial layer, and allowed to fold under the influence of the surface tension of the molten solder. This strategy is sketched in Figure 1.

We experimented with many different materials, structures, and processes. Figure 2 shows scanning electron microscopy (SEM) images of folded metallic polyhedra and the 2D precursors of these structures. The metallic faces of the polyhedra contained either holes (the trigonal pyramid in Fig. 2) or solid faces (as seen in the tetragonal pyramid, cube, and hexagonal prism). The faces ranged in size between 100–300 μm (on a side). The 2D precursors contained faces that were not hinged; the faces were aligned as close to each other as possible (given the mask and photolithographic capabilities). For 200–300 μm faces, spacings between 8 and 15 μm worked well; for 100 μm faces, a spacing of 8 to 10 μm was required. When the 2D structures were dipped in solder, the solder bridged the faces and formed a continuous layer. The 2D precursors were released from the wafer by dissolving a sacrificial layer on which they were built. The precursors were heated above the melting point of the solder. The liquid solder tried to minimize its surface area (capillarity); this process drew the faces together to form a compact 3D polyhedron. The equilibrated 3D polyhedron was, at this point, filled with solder; the folding thus worked best when the volume of the solder present was equal to the volume of the polyhedron.

Since the volume of solder present was equal to that deposited on the 2D precursor, the critical step controlling the yield of the process was the deposition of solder. We controlled the amount of solder deposited by changing the surface tension of the liquid solder, as well as by changing the solder–copper interfacial energy.[21] The surface tension of liquids decreases approximately linearly with increasing temperatures;[22] as a result, when the solder dip-coating was carried out at elevated temperatures (100 °C for a solder with melting point, m.p., 47 °C), a smaller volume of solder was deposited. The solder–copper interfacial energy was also controlled using fluxes and acids that aid in cleaning organic contaminants and dissolving oxide layers at the solder and copper surfaces. When the con-

[*] Prof. G. M. Whitesides, Dr. D. H. Gracias, V. Kavthekar, J. C. Love, K. E. Paul
Department of Chemistry and Chemical Biology, Harvard University
Cambridge, MA 02138 (USA)
E-mail: gwhitesides@gmwgroup.harvard.edu

[**] This work was funded by the National Science Foundation CHE-9901358 and the Defense Advanced Research Projects Agency/Space and Naval Warfare System Center, San Diego. J. C. Love thanks the U.S. Department of Defense for a graduate fellowship. The authors thank Hongkai Wu, Pascal Deschatelets, and Osahon Omoregie for helpful suggestions.

  0935-9648/02/0302-0235 $ 17.50+.50/0

ADVANCED MATERIALS

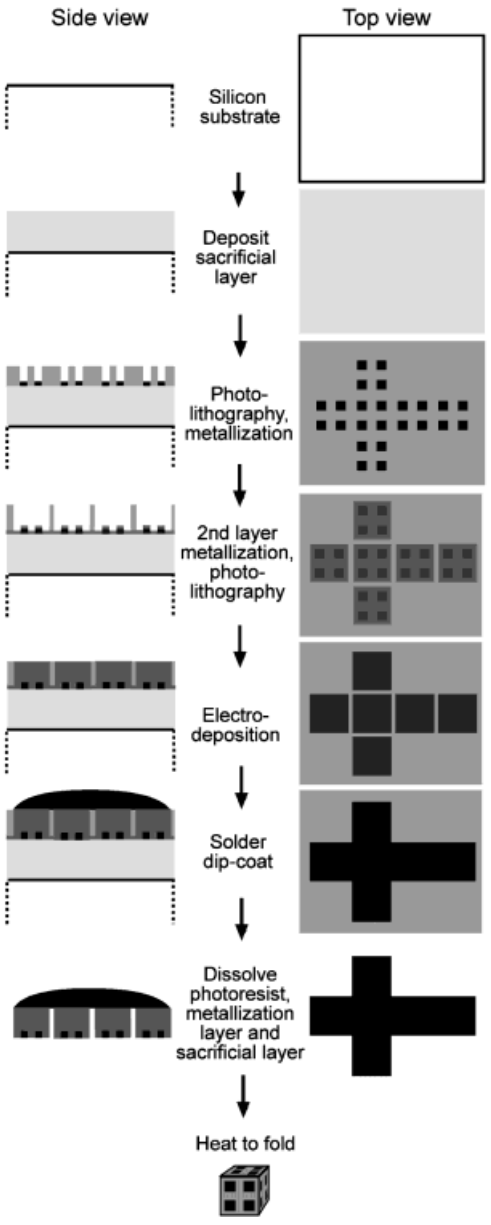

Fig. 1. The figure is a schematic of the basic steps involved in the fabrication of patterned polyhedra. The diagram is not drawn to scale. The steps include a) depositing a sacrificial layer on a silicon substrate, b) defining the pattern by photolithography followed by evaporation of a metallic layer, c) dissolving the first layer of photoresist, evaporating a seed layer of metal for electrodeposition, and patterning a second layer of photoresist with the boundary of each face of the polyhedron in registry with the pattern already present, d) electrodeposition to build each face, e) solder deposition by dip-coating, f) dissolution of photoresist, metallization layers, and sacrificial layer to release the structure from the substrate, g) heating the 2D structure above the melting point of the solder which causes it to fold into a 3D polyhedron, due to minimization of the surface area of the molten solder.

ditions were optimized, the solder volume coating the structures could be controlled sufficiently to give reproducible, well-defined polyhedra.

The yields of the correctly folded process also depended on the number of faces in the polyhedron, and on the symmetry of the 2D precursor relative to the final polyhedron—high yields (~90 %) were achieved for highly symmetric polyhedra with few faces (cubes and pyramids), while the yields were lower (~25 %) for the hexagonal prism. This trend in yields can be rationalized by observing that the 2D precursor needs to go through a series of geometrical transformations (that can be characterized by R—rotations, S—reflections, and T—translational operators) to form the final 3D polyhedron. The larger the number of transformations, the larger is the error associated with the process. For a given polyhedron, (a cube with six faces), there were a number of ways in which the structure could be aligned in the 2D precursor (as a cross, or in a straight line). In our experiments we found that auto-folding worked better for precursor structures that required fewer transformations to go from the precursor to the cube—the 2D precursor (with six square faces) in the shape of a cross (six transformations: 5R + 1T) works better than one shaped in a straight line (eight transformations: 5R + 3T).

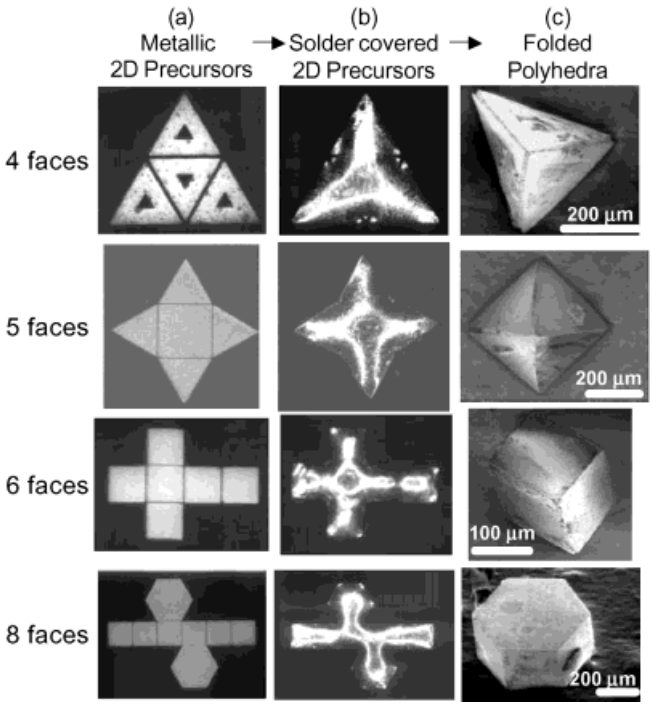

Fig. 2. a) Optical photographs of metallic 2D structures prior to folding. b) 2D precursors after dip-coating with solder. c) SEM images of polyhedra with bare metallic faces, ranging in size from 100 to 300 μm on a side.

In order to make functional polyhedra (i.e., polyhedra that could be used as 3D sensors or components for self-assembly), it is important to be able to pattern the surfaces of the polyhedra. We fabricated polyhedra with arbitrary patterns by incorporating an extra step of photolithography into the process of fabrication. As a demonstration, we fabricated a cube with a pattern of four squares on the surface of their faces and a trigonal pyramid with the letter H on each face. The patterns were built as the first layer on the substrate using photolithography and evaporation. A second step of photolithography was required to register this pattern to the boundary of the faces that were electrodeposited in a subsequent step. Figure 3a–c shows pictures of 200 μm side patterned polyhedra.

  0935-9648/02/0302-0236 $ 17.50+.50/0

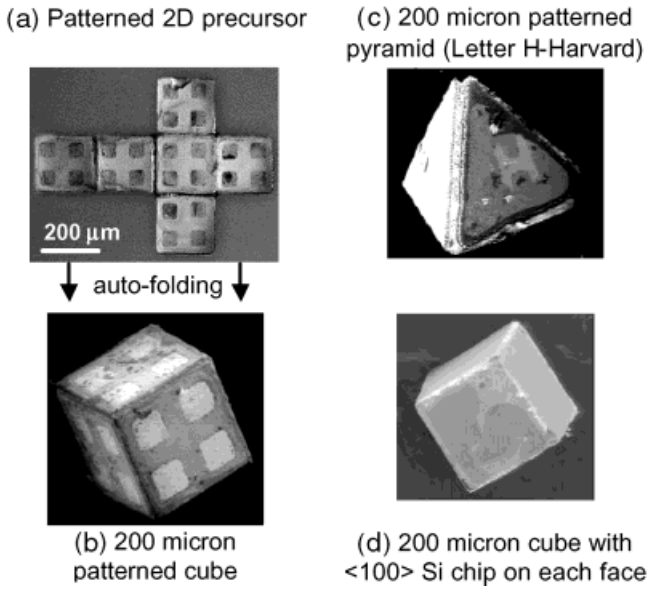

Fig. 3. a) Optical microscopy image of a 2D cross, the pattern shown is a contrast between Cr and Au. b) SEM image of a patterned, 200 μm (a side), metallic cube. c) SEM image of a 200 μm (a side), patterned metallic pyramid. d) SEM image of a 200 μm (a side), metallic cube containing 340 nm thick ⟨100⟩ silicon chips on each face.

The patterns shown are made of metal and were made by evaporation; we have made patterns with Cr, Ti, and Au. The strategy used is general enough that it can be implemented to build patterns of any material that can be evaporated or electrodeposited.

As a first step towards incorporating microelectronic devices on the faces of the polyhedra, we fabricated cubes (200 μm a side) with faces containing 340 nm thick Si ⟨100⟩ chips. (Fig. 3d). The cubes were built with silicon on insulator (SOI) wafers, where the topmost device layer was incorporated into the face of the cube. The buried oxide (BOx) layer (silicon dioxide) was used as the sacrificial layer. A metallic face was built over the silicon chip. When the faces folded into a cube, they pulled the silicon chips along with them. The cube shown has silicon chips on the exterior of each face; the inner side of the face is made of nickel.

In conclusion, these results demonstrate a new strategy for fabricating small, 3D, polyhedral structures based on existing 2D microfabrication technology (to make a planar precursor), and self-folding based on surface tension to fold that structure into the final 3D form. The patterns of four squares on each face of the cube in Figure 3 resemble a 2 × 2 array of connectors. In the future, it may be possible to assemble such cubes using solder-based self-assembly to form micrometer-scale 3D aggregates.[1,23] Finally, we have built structures with silicon single crystal chips on each face. Single crystal silicon (along with dopants) provides the route for fabricating most electronic components (e.g., transistors) in current integrated circuit technology.[24] Polyhedra with single crystal silicon faces may eventually provide a framework for building 3D electronic device modules (i.e., on the faces of polyhedra) for 3D, self-assembled, electronic systems.

Experimental

We fabricated three kinds of polyhedra: A) polyhedra with bare metallic faces, B) polyhedra with patterned metallic faces, and C) polyhedra with silicon chips on each face. The following materials and processes were used for fabricating the above-mentioned polyhedra A, B, and C.

Substrates: We used ⟨100⟩ test grade silicon wafers (Silicon Sense, www.siliconsense.com) as our substrates for fabricating polyhedra A and B. We used SOI wafers (340 nm ⟨100⟩ Si, 400 nm BOx thickness, SOITEC, www.soitec.com) as our substrates for fabricating C.

Sacrificial Layer: To fabricate polyhedra A and B, we used a sacrificial layer that was either 1) thermally grown silicon dioxide (150–200 nm) or 2) spin-on glass (Accuglass-Honeywell, www.electronicmaterials.com); the thickness of this layer could be controlled between 300 and 500 nm. For polyhedra C, the BOx layer of the SOI wafer functioned as the sacrificial layer.

Photolithography: Masks for photolithography were either fabricated using a high-resolution printer (Herkules Imagesetter; Pageworks, www.pageworks.com) or 16 mm microfilm using a camera with 24× reduction (New England Micro Graphics, www.nemicrographics.com). The masks fabricated by the printer are cheaper than those made by microfilm, however the smallest feature possible with the printer is ~15 μm compared to ~8 μm for the microfilm. We used two kinds of photoresists for fabricating polyhedra B: 1) Thin photoresist: Shipley 1813, 1.5 μm thick, and 2) thick photoresist: Shipley SJR 5440, 4.4 μm thick (Microchem, http://microchem.com). Shipley 1813 is easy to process and was used to pattern the substrates prior to the evaporation process; this photoresist however degrades in electrodeposition baths. Shipley 5440 is more difficult to process, however it is stable in nickel and copper electrodeposition baths and was used to pattern substrates prior to electrodeposition. For polyhedra A and C we used only one photoresist, i.e., Shipley SJR 5440.

We used two photolithographic steps to fabricate 2D precursors of polyhedron B: we did the first layer of photolithography to define the pattern on each face of the polyhedron and then another layer of photolithography (with registry to alignment marks on the first layer) to define the boundary of each face. For polyhedra A and C the first layer of photolithography was eliminated.

Evaporation: For all polyhedra it was necessary to evaporate a metallic seed layer (3 nm Cr/17 nm Au) to make the wafer electrically conductive for electrodeposition. This step was done prior to photolithography using SJR 5440. For polyhedra B an additional evaporation step (Cr/Au or Cr/Ti) was required after the first layer of photolithography to define the pattern on each face of the polyhedron. This step was followed by dissolution of the thin photoresist in acetone, i.e., lift-off.

Electrodeposition: The faces of all polyhedra were fabricated by electrodepositing Ni (~3 μm thick) using a commercial nickel bath (nickel sulfamate RTU bath, Technic, Inc, www.technic.com) at 50 °C. Our choice of nickel was stimulated by the fact that a) nickel is cheap and easy to electrodeposit and b) nickel is paramagnetic—this means that the structures formed can be manipulated and separated by magnetic fields. 1 μm of copper was subsequently electrodeposited from a commercial copper bath (Copper U, Technic, Inc.) onto the nickel to facilitate wetting of the faces by solder. (The solder used does not wet nickel well.) All electrodeposition was done at 1–2 mA/cm^2, and the heights of the structures were measured using surface profilometry. The final height of the faces (~4 to 5 μm) was similar to the height of Shipley 5440 photoresist (4.4 μm).

Solder Deposition: The wafer was dipped in molten solder (two bismuth alloys were compatible with the process; m.p. ~ 47 °C or m.p. 70 °C, Small Parts, Inc., www.smallparts.com) containing liquid fluxes such as conc. HCl and 1429 water soluble flux, Kester, www.kester.com). The solder bridged the faces of the 2D precursor. The solder deposition was carried out either while the photoresist was still present in between the metallic faces or after it had been stripped and the underlying metallic seed layers had been dissolved. Since the photoresist provided support for the solder between adjacent faces, faces separated by larger distances could be bridged when solder deposition was carried out prior to photoresist removal. In the case of polyhedron C, however, it was necessary to dissolve the photoresist and underlying layers prior to solder deposition. Dissolution was necessary in order to reach the silicon layer that was then etched to define the boundary of the silicon chip on each face of the polyhedron. The solder deposition was carried out after etching the silicon layer in between pieces. The solder bridged adjacent faces, however the distances between faces needed to be as small as possible, e.g., 8 μm for 200 μm faces.

Dissolution and Etching: For polyhedra A and B, dissolution and etching were carried out after solder deposition, for C, dissolution and etching were done prior to solder deposition. The photoresist was dissolved by sonication in acetone to expose underlying metallic seed layers. The metallic layers of Cr/Au were dissolved in an etchant that consisted of 0.044 g potassium ferrocyanide, 0.33 g potassium ferricyanide, 5.6 g potassium hydroxide, 2.48 g sodium thiosulfate in 100 mL water. Etch times were ~15 min. For polyhedron C, the underly-

  0935-9648/02/0302-0237 $ 17.50+.50/0

ADVANCED MATERIALS

ing ⟨100⟩ silicon layer on the SOI wafer was etched for 1 min (1 min is long enough to etch vertically through 340 nm of Si, without much undercutting) in a commercial silicon etchant (silicon, preferential ⟨100⟩ etchant, PSE-300, Transene CO Inc, www.transene.com).

Structure Release and Folding: The structures were released by dissolving the sacrificial layer in commercial SiO_2 etchant (fluoride–bifluoride improved buffer HF, Transene CO Inc, www.transene.com). After rinsing in the SiO_2 etchant and acetone, we transferred the 2D structures to an acidified aqueous solution (HCl, ~ pH 1, a drop of surfactant (Triton X-100, Aldrich, http://www.aldrich.com) was added to minimize the formation of bubbles) and heated above the melting point of the solder. Auto-folding occurred above the m.p. of the solder on the time scale of a second. The folded structures were picked up with a magnetic tape and imaged with an SEM.

Received: September 3, 2001
Final version: October 26, 2001

[1] D. H. Gracias, J. Tien, T. L. Breen, C. Hsu, G. M. Whitesides, *Science* **2000**, *289*, 1170.
[2] M. J. Madou, *Fundamentals of Microfabrication*, CRC Press, Boca Raton, FL **1997**.
[3] G. Kovacs, *Micromachined Transducers Sourcebook*, McGraw-Hill, New York **1998**.
[4] M. L. Schattenburg, J. Carter, W. Chu, R. C. Fleming, R. A. Ghanbari, M. Mondol, N. Polce, H. I. Smith, *Mater. Res. Soc. Symp. Proc.* **1993**, *306*, 63.
[5] Y. Xia, G. M. Whitesides, *Angew. Chem. Int. Ed.* **1998**, *37*, 550.
[6] J. G. Goodberlet, *Appl. Phys. Lett.* **2000**, *76*, 667.
[7] A. Ishikawa from Ball Semiconductor (http://www.ballsemi.com), *US Patent 6 069 682*, **2000**.
[8] H. Suzuki, N. Ohya, N. Kawahara, M. Yokoi, S. Ohyanagi, T. Kurahashi, T. Hattori, *J. Micromech. Microeng.* **1995**, *5*, 36.
[9] S. A. Campbell, *The Science and Engineering of Microelectronic Fabrication*, Oxford University Press, New York **1996**.
[10] K. S. J. Pister, M. W. Judy, S. R. Burgett, R. S. Fearing, *Sens. Actuators A* **1992**, *33*, 249.
[11] K. Suzuki, I. Shimoyama, H. Miura, *J. Microelectromech. Syst.* **1994**, *3*, 4.
[12] R. R. A. Syms, *IEEE Photon. Technol. Lett.* **2000**, 1507.
[13] R. R. A. Syms, S. Blackstone, *Proc.—Electrochem. Soc.* **2001**, *99*, 415.
[14] P. W. Green, R. R. A. Syms, E. M. Yeatman, *J. Microelectromech. Syst.* **1995**, *4*, 170.
[15] K. F. Harsh, V. M. Bright, Y. C. Lee, *Sens. Actuators A* **1999**, *3*, 237.
[16] K. F. Harsh, V. M. Bright, Y. C. Lee, *Proc.—Electron. Comp. Technol. Conf.* **2000**, *50*, 1690.
[17] E. E. Hui, R. T. Howe, M. S. Rodgers, presented at *IEEE 13th Int. Conf. on Micro Electro Mechanical Systems*, Miyazaki, Japan, January 23–27, **2000**.
[18] E. Smela, O. Inganas, I. Lundstrom, *Science* **1995**, *268*, 1735.
[19] E. W. H. Jager, E. Smela, O. Inganas, *Science* **2000**, *290*, 1540.
[20] T. Ebefors, E. Kalvesten, G. Stemme, *J. Micromech. Microeng.* **1998**, *8*, 188.
[21] J. Hwang, *Modern Solder Technology for Competitive Electronics Manufacturing (Electronic Packaging and Interconnection)*, McGraw-Hill, New York **1996**.
[22] G. A. Somorjai, *Introduction to Surface Chemistry and Catalysis*, Wiley, New York **1994**.
[23] N. B. Bowden, M. Weck, I. S. Choi, G. M. Whitesides, *Acc. Chem. Res.* **2001**, *34*, 231.
[24] P. B. Griffin, J. D. Plummer, M. D. Deal, *Silicon VLSI Technology: Fundamentals, Practice and Modeling*, Prentice-Hall, Englewood Cliffs, NJ **2000**.

Gold Nanoparticle/Polyphenylene Dendrimer Composite Films: Preparation and Vapor-Sensing Properties**

By *Tobias Vossmeyer*,* *Berit Guse*, *Isabelle Besnard*, *Roland E. Bauer*, *Klaus Müllen*, and *Akio Yasuda*

During the past few years, thin-film materials comprising ligand-stabilized metal nanoparticles have attracted considerable attention.[1–7] Since the preparation of such films allows the combination of various organic molecules with a variety of nanoparticle cores, it may be possible to "tailor" their overall physical and chemical properties for specific applications. For the following reasons, the use of composite metal nanoparticle/organic films for chemical sensing is especially interesting. First, by combining the nanoparticles with suitable organic compounds it is possible to control the chemical nature of the film material, and thereby the selectivity of the sensor device, while the physical properties of the nanoparticles can be utilized for signal transduction. Second, because of the high surface-to-volume ratio of nanoparticle-based materials, a significant number of the atoms are located at interfaces. Therefore, the overall materials' properties are dominated by surface properties, which can be strongly affected by the interaction with analyte molecules. Third, nanoparticle films can be prepared as highly porous materials, which allow the diffusion of analyte molecules within the film and, thus, support the efficient uptake of analyte species. Recently, Willner and co-workers[8–10] described the use of gold nanoparticle/cyclophane composite films as electrodes for the selective electrochemical detection of redox-active analytes in the liquid phase. Wohltjen and Snow[11] demonstrated that films prepared from octanethiol-stabilized gold-nanoparticle solutions via solvent evaporation could be used as vapor-sensing chemiresistors. Later, Evans et al.[12] extended this approach by using *para*-functionalized thiophenol ligands to control the chemical selectivity of such sensors. We report here on the layer-by-layer assembly of mechanically reinforced, cross-linked gold nanoparticle/polyphenylene dendrimer (GNPD) films and their use as vapor-sensing chemiresistors. In particular, we chose hydrophobic polyphenylene dendrimers to enhance the sensitivity to volatile organic compounds (VOCs) and to suppress undesired cross-sensitivity to humidity. More-

[*] Dr. T. Vossmeyer, B. Guse, Dr. I. Besnard, Dr. A. Yasuda
Materials Science Laboratories
Advanced Technology Center Stuttgart
Sony International (Europe) GmbH
Heinrich-Hertz-Strasse 1, D-70327 Stuttgart (Germany)
R. E. Bauer, Prof. K. Müllen
Max-Planck-Institut für Polymerforschung
Ackermannweg 10, D-55128 Mainz (Germany)

[**] We thank Dr. N. Matsuzawa, (Sony International (Europe) GmbH, Materials Science Laboratories) and Dr. M. Enomoto (Sony Corporation, Fusion Domain Laboratories) for helpful discussions. This project was partly supported by the BMBF, FKZ 03C0302A, and FKZ 03C0299.

  0935-9648/02/0302-0238 $ 17.50+.50/0